

RESEARCH ARTICLE

AMG232 inhibits angiogenesis in glioma through the p53–RBM4–VEGFR2 pathway

Yao Xiao*, Mingliang Li*, Teng Ma, Hao Ning and Libo Liu[†]

ABSTRACT

AMG232 effectively inhibits cancers with wild-type p53 (also known as TP53) by reactivating p53, but whether it inhibits glioma angiogenesis remains unclear. This study confirms that AMG232 inhibits the proliferation of glioma endothelial cells (GECs) in a dose-dependent manner and inhibits the angiogenesis of GECs. p53 and RNA-binding motif protein 4 (RBM4) were expressed at low levels in GECs, while MDM2 and vascular endothelial growth factor receptor 2 (VEGFR2, also known as KDR) were highly expressed. *In vitro* and *in vivo* experiments confirmed that AMG232 upregulated p53 and RBM4, and downregulated MDM2 and VEGFR2 by blocking the MDM2–p53 interaction. Both p53 silencing and RBM4 silencing significantly upregulated the expression of VEGFR2, promoted the proliferation, migration and tube formation of GECs, and reversed the effects of AMG232 on downregulating VEGFR2 and inhibiting the angiogenesis of GECs. AMG232 increased RBM4 expression by upregulating p53, and p53 bound to RBM4 and promoted its transcription. RBM4 bound to and shortened the half-life of VEGFR2, promoting its degradation. Finally, AMG232 produced a significant decrease in new vessels and hemoglobin content *in vivo*. This study proves that AMG232 inhibits glioma angiogenesis by blocking the MDM2–p53 interaction, in which the p53–RBM4–VEGFR2 pathway plays an important role.

KEY WORDS: AMG232, p53, RBM4, VEGFR2, Glioma, Angiogenesis

INTRODUCTION

Glioma is a common intracranial tumor and one of the most malignant brain tumors in humans, with low survival rate and high mortality (Reifenberger et al., 2017). Despite great progress in tumor treatment, such as surgery, radiotherapy and chemotherapy, glioma patients still have a poor prognosis (Xu et al., 2020). Molecular targeted therapy has become an important method for treating glioma. In the process of tumor development, the normal static vascular system constantly sprouts new blood vessels to help maintain the expansion of tumor growth (Hanahan and Weinberg, 2011). Glioma is a vascular-rich tumor, and angiogenesis plays an important role in its occurrence, development and recurrence (Ma et al., 2017). Vascular endothelial growth factor (VEGF) is the most abundant and important angiogenic protein in glioma (Carvalho et al., 2021). Vascular endothelial growth factor receptor 2 (VEGFR2, also known as KDR), a tyrosine kinase

receptor, is mainly expressed in endothelial cells and their embryonic precursor cells, and is essential for angiogenesis of tumor endothelial cells (Shibuya, 2013).

AMG232 is the most effective inhibitor currently known of mouse double minute 2 (MDM2). It can block the interaction between MDM2 and p53 (also known as TP53) and is currently undergoing clinical trials (Konopleva et al., 2020). Studies have demonstrated that the MDM2–p53 interaction plays an important role in cancer prevention and treatment (Qin et al., 2018). As a tumor suppressor, p53 plays a major role in controlling the occurrence and development of cancer by regulating cell cycle arrest, apoptosis, senescence and DNA repair (Sabapathy and Lane, 2019). About 50% of human tumors contain a mutant *TP53* gene, and mutant p53 is an oncogene (Olivier, et al., 2010). In the remaining tumors, p53 is wild-type, but its full activation and function may be blocked by other proteins, such as MDM2, etc. (Oliner et al., 1992). MDM2 oncogene is located at 12q13-14 and is the main negative regulator of p53 (Juven-Gershon and Oren, 1999). It can target p53 for ubiquitylation and degradation by the proteasome, resulting in low expression of p53 in tumor cells. It can also block the binding of p53 to its targeted DNA by interacting with p53 and can reduce the transcriptional capacity of p53. Meanwhile, MDM2 promotes the export of p53 from the nucleus, further reducing the transcriptional capacity of p53 (Canon et al., 2015; Freedman et al., 1999; Haupt et al., 1997). AMG232 binds MDM2 protein with picomole affinity and blocks the MDM2–p53 interaction, thereby enhancing the activity of p53 and inducing cytotoxicity (Oliner et al., 1992). In glioma, varying severities of p53 mutation can exist (Cohen and Colman, 2015). Compared with p53 mutant glioma, AMG232 is more effective in glioma containing wild-type p53 and significantly inhibits the stemness of p53 wild-type glioblastoma stem cells (Her et al., 2018). However, whether AMG232 can regulate angiogenesis of glioma has not been reported.


Studies have shown that adducin 3 (ADD3) inhibits p53 expression and promotes glioma angiogenesis through a VEGF–VEGFR2-mediated pathway (Kiang et al., 2020), suggesting that AMG232 may upregulate p53 expression by blocking MDM2–p53 interaction, thereby inhibiting glioma angiogenesis. It has been reported that mutant p53 binds near the transcription start site (TSS) of the VEGFR2 promoter and influences its transcription through interacting with the SWI/SNF complex, thereby regulating breast cancer cell function (Pfister et al., 2015). However, it has not been reported whether wild-type p53 can regulate VEGFR2 expression. We found no wild-type p53-binding site in the VEGFR2 promoter region through JASPAR analysis (<https://jaspar.genereg.net>), suggesting that p53 regulates the expression of VEGFR2 through an indirect pathway and affects glioma angiogenesis.

RNA-binding proteins (RBPs) are key components in RNA metabolism and regulate all aspects of RNA biogenesis, from RNA maturation and nucleoplasmic transport to subcellular localization, translation and RNA degradation (Gebauer et al., 2021). RBPs can interact with target RNA in a sequence- and structure-dependent

Department of Neurobiology, School of Life Sciences, China Medical University, Shenyang 110122, People's Republic of China.

*These authors contributed equally to this work

[†]Author for correspondence (liulibo77@163.com)

 T.M., 0000-0003-1450-7585; L.L., 0000-0001-6453-7403

Handling Editor: John Heath

Received 27 May 2022; Accepted 21 December 2022

manner through their unique RNA-binding domains to promote or inhibit the stability and expression of target RNA (Majumder and Palanisamy, 2020). The RNA-binding motif protein 4 gene (*RBM4*), which is located in 11q13.2, is a multifunctional RNA-binding protein that plays an important role in mRNA alternative splicing and translation control (Huangfu et al., 2020). *RBM4* inhibits tumor development by inhibiting the proliferation, migration and invasion of various cancer cells (Wang et al., 2020). Chang et al. reported that *RBM4* affects *VEGFR2* expression and regulates lung cancer endothelial cell function by regulating the expression of HIF-1 α -ex14, an isoform of hypoxia-inducible factor 1 α (HIF1 α) (Chang and Lin, 2019), and suggested that *RBM4* may have the function of regulating tumor blood vessels. However, the role of *RBM4* in glioma and glioma angiogenesis remains unclear. Can *RBM4* regulate the expression of *VEGFR2* in the same way as RBPs? To investigate this, we used bioinformatics software RBPmap (<https://rbpmap.technion.ac.il/>) to predict and analyze the existence of binding sites between *RBM4* and *VEGFR2*, suggesting that *RBM4* may influence *VEGFR2* expression by regulating its stability, thereby regulating glioma angiogenesis.

As an important tumor suppressor, p53 can act as a transcription factor to regulate the transcription of dozens of target genes with multiple biological functions to inhibit tumor growth (Li et al., 2021). It can exert both transcriptional activation and transcriptional inhibition effects (Gonzalez-Rellan et al., 2021; Wu et al., 2019). However, it is not clear whether p53 can transcriptionally regulate the expression of *RBM4*. Bioinformatics software JASPAR predicts that there are transcriptional binding sites of p53 within 2000 bp upstream of the *RBM4* TSS, suggesting that p53 can regulate the expression of *RBM4* through transcription, which in turn regulates the expression of *VEGFR2* and affects glioma angiogenesis.

In this study, we have focused on the endogenous expression of p53, MDM2, *RBM4* and *VEGFR2* in glioma endothelial cells (GECs). We further explore the effects and molecular mechanisms of AMG232 in regulating glioma angiogenesis through the above molecules. The aim of this study was to prove that AMG232 can inhibit glioma angiogenesis by blocking the MDM2–p53 interaction, thereby inhibiting the malignant progression of glioma and providing promising targets for glioma therapy.

RESULTS

AMG232 inhibits the proliferation, migration and tube formation of GECs

A CCK-8 assay was used to detect the effect of AMG232 on the proliferation of GECs at different concentrations and different time points. As shown in Fig. 1A, compared with the control group, there was no statistical difference in the effect of DMSO on GEC viability at 24 h, 48 h and 72 h. Compared with the DMSO group, the cell viability of GECs treated with 0.5 μ M, 1 μ M, 2 μ M, 4 μ M and 8 μ M AMG232 for 24 h, 48 h and 72 h decreased gradually as the concentration increased. The cell viability of GECs was not significantly changed by treatment with 0.5 μ M AMG232 for 24 h, 48 h and 72 h. The cell viability of GECs was significantly decreased after treatment with 1 μ M AMG232 for 24 h and 48 h, and there was no statistical change at 72 h. The cell viability of GECs was significantly decreased by treatment with 2 μ M, 4 μ M and 8 μ M AMG232 for 24 h, 48 h and 72 h; the decrease produced by 8 μ M AMG232 was more significant. The IC_{50} of AMG232 acting on GECs was further calculated, and the results showed that the IC_{50} values for AMG232 after 24 h, 48 h and 72 h of treatment

were 4.1 μ M, 3.9 μ M and 4.3 μ M, respectively (Fig. 1B). Therefore, normal human brain microvascular endothelial cells (ECs) were cultured with U87-conditioned medium for 24 h to form GECs, and then 3.9 μ M AMG232 was added for 48 h for subsequent studies (Fig. 1C). As shown in Fig. 1D–F, after treatment with 3.9 μ M AMG232 for 48 h, the cell viability and migration ability of GECs were significantly decreased; meanwhile, the branch numbers and tube lengths were significantly reduced, suggesting that AMG232 could significantly inhibit angiogenesis of GECs.

AMG232 regulates the expression of p53, MDM2 and VEGFR2 in GECs

The mRNA and protein expression levels of p53, MDM2 and *VEGFR2* in ECs and GECs were detected by qRT-PCR and western blot assays. As shown in Fig. 2A, compared with the ECs group, the mRNA and protein expression levels of p53 were significantly decreased in GECs, while the mRNA and protein expression levels of MDM2 and *VEGFR2* were significantly increased in GECs (Fig. 2B,C). As shown in Fig. 2D, compared with the control group, the mRNA and protein expression levels of p53 were significantly increased in GECs after AMG232 treatment, whereas the mRNA and protein expression levels of MDM2 and *VEGFR2* were significantly decreased in GECs after AMG232 treatment (Fig. 2E,F). These results demonstrated that in GECs, p53 expression was low, whereas expression of MDM2 and *VEGFR2* was high. AMG232 significantly upregulated the expression of p53 and downregulated the expression of MDM2 and *VEGFR2* by blocking the MDM2–p53 interaction.

AMG232 inhibits glioma angiogenesis by upregulating the expression of p53

In order to further clarify the role of p53 in the regulation of glioma angiogenesis by AMG232, p53-silenced GECs were constructed through stable transfection of p53 silencing plasmids. The silencing efficiency of p53 was detected and verified by qRT-PCR and western blot assays (Fig. 3A). As shown in Fig. 3B, the results of qRT-PCR and western blot assays showed that there was no statistical difference between the silencing negative control (sh-NC) group and the untreated control group. Compared with the sh-NC group, the mRNA and protein expression levels of *VEGFR2* in GECs in the p53-silenced (sh-p53) group were significantly increased. Compared with the AMG232-treated group, the mRNA and protein expression levels of *VEGFR2* in GECs in the AMG232-treated p53-silenced (AMG232+sh-p53) group were significantly increased. Compared with the sh-p53 group, the expression levels of *VEGFR2* in GECs in the AMG232+sh-p53 group were significantly decreased. The above results suggest that p53 silencing significantly upregulates *VEGFR2* expression and reverses the effect of AMG232 on downregulation of *VEGFR2* expression; that is, AMG232 can downregulate *VEGFR2* expression by upregulating p53.

Similarly, as shown in Fig. 3C–E, compared with the control group, there were no significant differences in cell viability, migration ability, branch numbers and tube lengths of GECs in the sh-NC group. Compared with the sh-NC group, the cell viability and migration ability of GECs in the sh-p53 group were significantly enhanced, and the branch numbers and tube lengths were significantly increased. Compared with AMG232 group, the cell viability and migration ability of GECs in AMG232+sh-p53 group were significantly enhanced, and the branch numbers and tube lengths were significantly increased. Compared with the sh-p53 group, the cell viability and migration ability of GECs in the

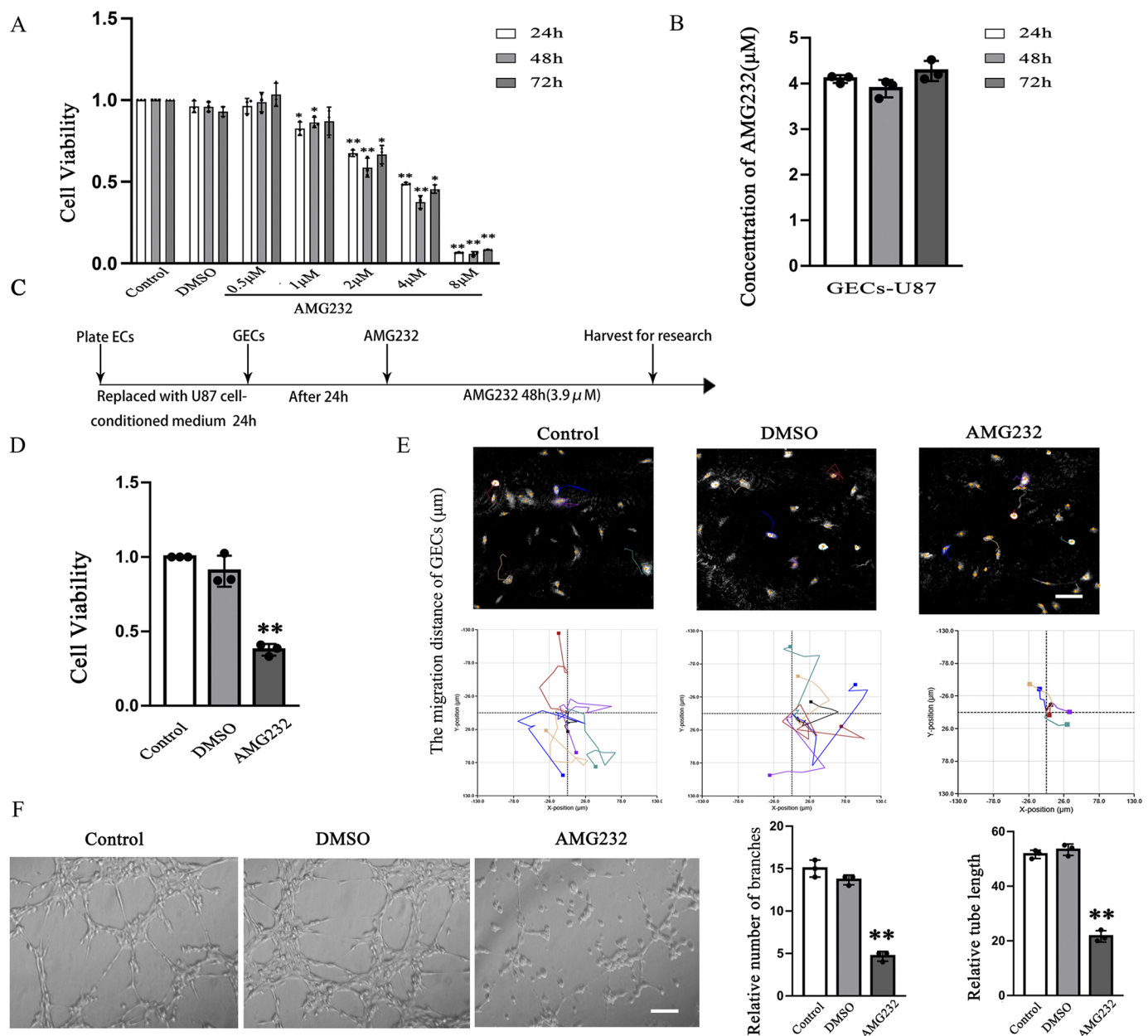


Fig. 1. Effects of AMG232 on the proliferation, cell viability, migration and tube formation of GECs. (A) A CCK-8 assay was used to detect the effects of AMG232 on the cell viability of GECs at different concentrations and at different times. Data are mean±s.d. ($n=3$ per group). * $P<0.05$ and ** $P<0.01$ versus DMSO group (one-way ANOVA with Tukey's multiple comparisons test). (B) IC_{50} was calculated according to the inhibition rate of AMG232 on GECs for 24 h, 48 h and 72 h detected by a CCK-8 assay. Data are mean±s.d. ($n=3$ per group). (C) A schematic of GECs acquisition and AMG232 administration. (D) A CCK-8 assay was used to detect the effect of $3.9 \mu\text{M}$ AMG232 on the cell viability of GECs. Data are mean±s.d. ($n=3$ per group). ** $P<0.01$ versus DMSO group (one-way ANOVA with Tukey's multiple comparisons test). (E) The Hstudio M4 system was used to observe the effect of AMG232 on the migration of GECs ($n=3$). Cell tracks over a period of 12 h are shown below the images, with the track start centered at the origin. Scale bar: $100 \mu\text{m}$. (F) A Matrigel tube formation assay was applied to determine the effect of AMG232 on the tube formation of GECs. Scale bar: $100 \mu\text{m}$. Quantification of number of branches and tube length is shown on the right as mean±s.d. ($n=3$ per group). ** $P<0.01$ versus DMSO group (one-way ANOVA with Tukey's multiple comparisons test).

AMG232+sh-p53 group were significantly reduced, and the branch numbers and tube lengths were significantly decreased. The above results suggest that p53 silencing significantly enhances the proliferation, migration and tube formation of GECs, and reverses the effect of AMG232 on inhibiting the proliferation, migration and tube formation of GECs. In conclusion, AMG232 can downregulate VEGFR2 expression by upregulating P53, thereby inhibiting the proliferation, migration and tube formation of GECs.

AMG232 upregulates p53, which in turn transcriptionally promotes the expression of RBM4

As shown in Fig. 4A, the expression levels of RBM4 in ECs and GECs were detected by qRT-PCR and western blot assays. The results showed that, compared with the ECs group, the mRNA and protein expression levels of RBM4 in GECs were significantly decreased. As shown in Fig. 4B, compared with the control group, the mRNA and protein expression levels of RBM4 in GECs were

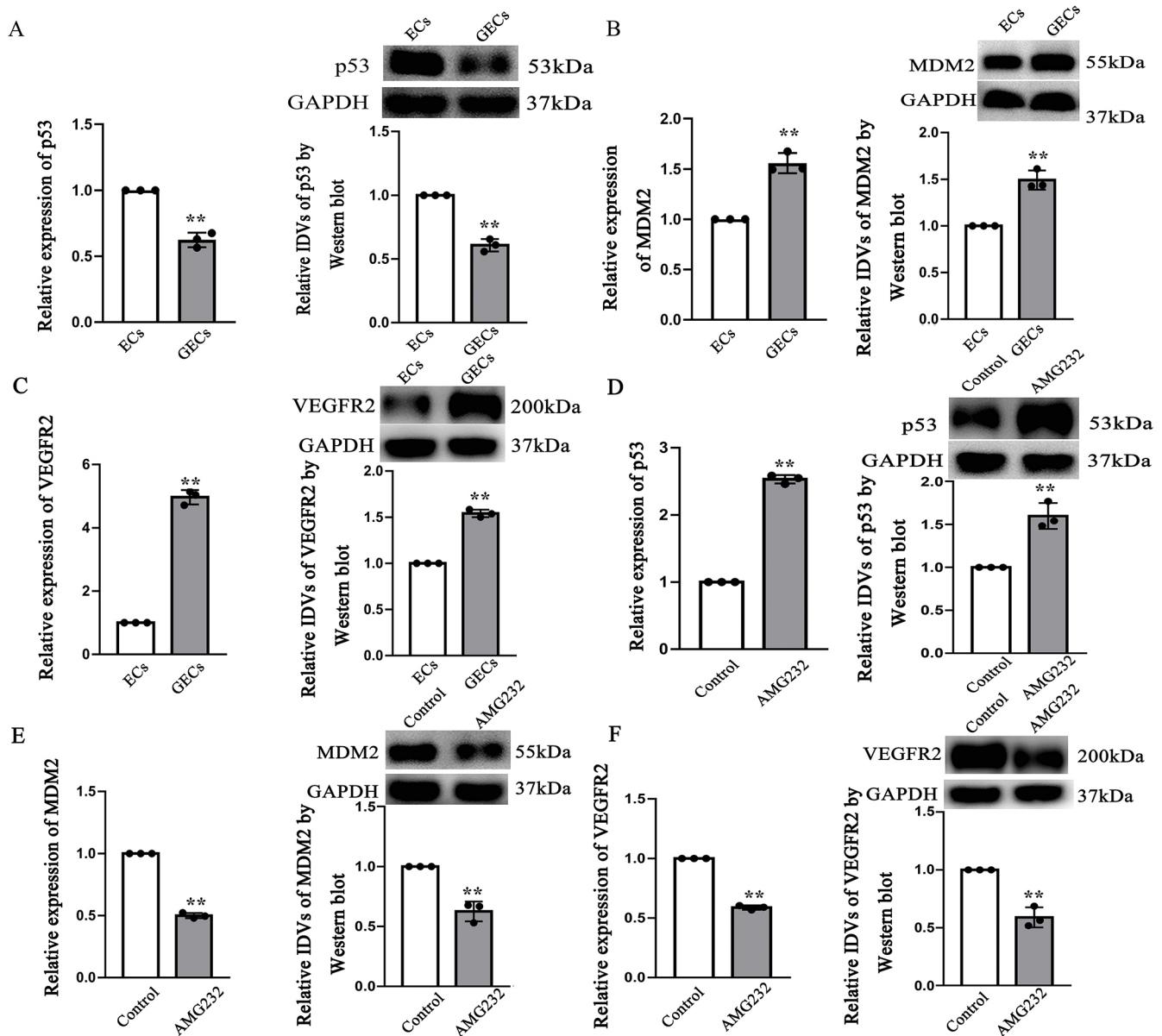


Fig. 2. The endogenous expression of p53, MDM2 and VEGFR2 in GECs, and the effect of AMG232 on their mRNA and protein expression. (A–C) qRT-PCR (left) and western blot assays (right) were used to detect the expression of (A) p53, (B) MDM2 and (C) VEGFR2. Data are mean±s.d. ($n=3$ per group), ** $P<0.01$ versus ECs group (two-tailed unpaired Student's t -test). (D–F) qRT-PCR (left) and western blot assays (right) were used to detect the mRNA and protein levels of (D) p53, (E) MDM2 and (F) VEGFR2 after AMG232 treatment. Data are mean±s.d. ($n=3$ per group), ** $P<0.01$ versus control group (two-tailed unpaired Student's t -test).

significantly increased after AMG232 treatment. Meanwhile, the results of qRT-PCR and western blot assays showed that mRNA and protein expression levels of RBM4 in the sh-p53 group were significantly lower than those in the sh-NC group. Compared with AMG232 group, the mRNA and protein expression levels of RBM4 in the AMG232+sh-p53 group were significantly decreased, while compared with the sh-p53 group, the expression levels of RBM4 in the AMG232+sh-p53 group were significantly increased (Fig. 4C). These results suggest that AMG232 can increase the expression of RBM4 in GECs by upregulating p53.

In order to study the possible mechanism by which p53 regulates the expression of RBM4, by searching JASPAR and UCSC (<http://www.genome.ucsc.edu/>) databases it was determined that there are two potential binding sites of p53 at 2000 bp upstream and 100 bp

downstream of RBM4 TSS. A ChIP assay was performed to verify whether p53 could bind to the promoter region of RBM4. The result of ChIP assay showed that IgG could not precipitate the RBM4 promoter sequence, and the negative control region did not recruit p53. Among the predicted binding sites, binding site 2 of RBM4 was recruited to p53, suggesting that the interaction of RBM4 with p53 was through this site (Fig. 4D). In order to further verify the binding relationship between p53 and RBM4, a dual-luciferase reporter gene assay was used. As shown in Fig. 4E, compared with the RBM4 5'-UTR-Wt+p53 overexpressed negative control [p53(+)]NC group, the luciferase activity in the RBM4 5'-UTR-Wt+p53 overexpressed [p53(+)] group was significantly reduced. Compared with the RBM4 5'-UTR-Mut1+p53(+)]NC group, the luciferase activity in the RBM4 5'-UTR-Mut1+p53(+)] group was

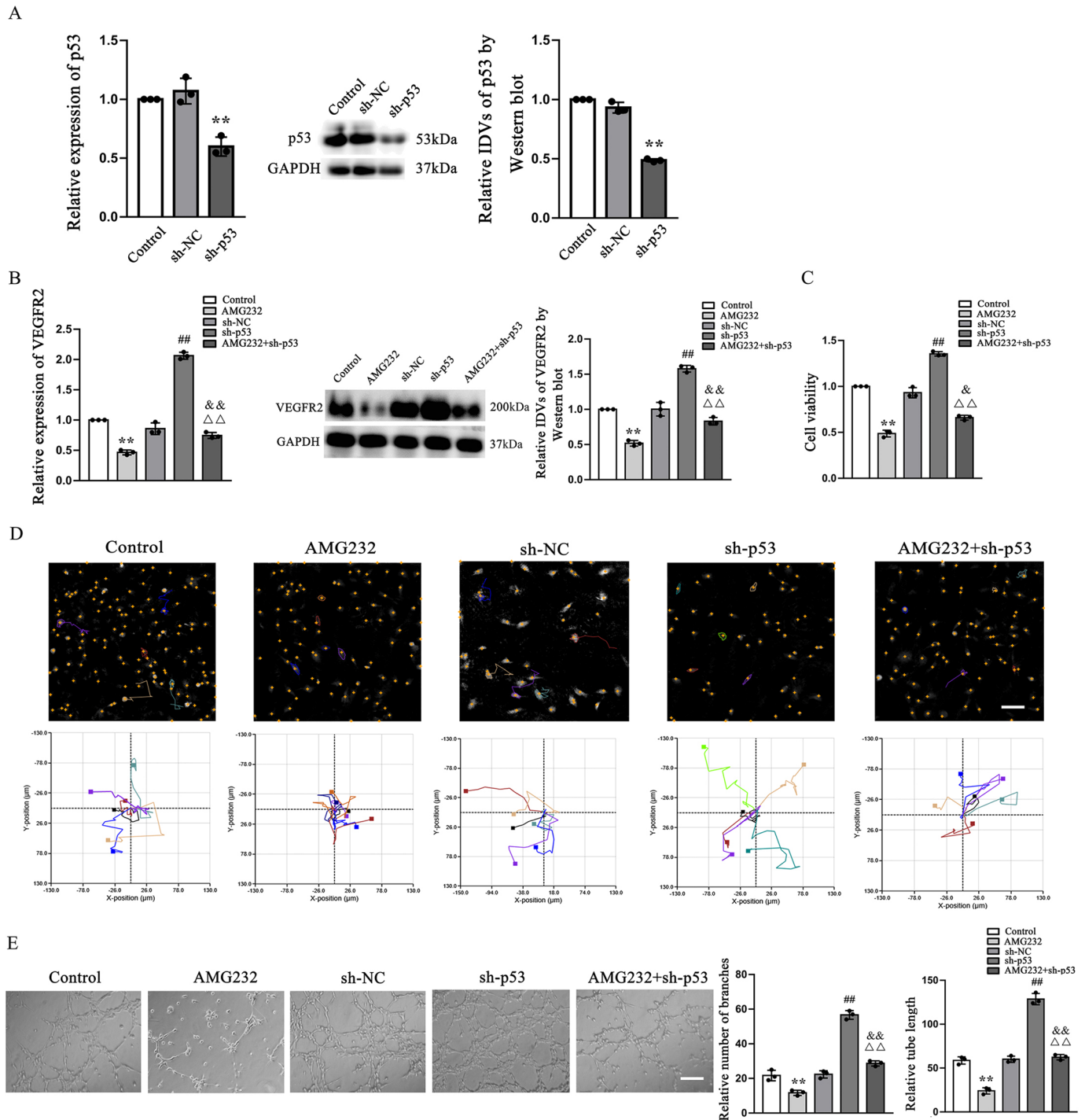


Fig. 3. The effects of p53 silencing on angiogenesis in GECs, and the role of p53 in the regulation of angiogenesis in GECs by AMG232. (A) The silencing efficiency of p53 was verified by qRT-PCR (left) and western blot (right) assays. Data are mean \pm s.d. ($n=3$ per group), $**P<0.01$ versus the sh-NC group (one-way ANOVA with Tukey's multiple comparisons test). (B) qRT-PCR (left) and western blot (right) assays were used to detect the mRNA and protein expression of VEGFR2. (C) A CCK-8 assay was used to detect the cell viability of GECs. (D) The Hstudio M4 system was used to observe the migration ability of GECs in the indicated groups ($n=3$). Cell tracks are shown below the images, with the track start centered at the origin. Scale bar: 100 μ m. (E) Matrigel tube formation assay was applied to determine the tube formation of GECs in the indicated groups. Scale bar: 100 μ m. Data in B, C and E are mean \pm s.d. ($n=3$ per group). $**P<0.01$ versus control group, $###P<0.01$ versus sh-NC group, $&P<0.05$ and $&&P<0.01$ versus AMG232 group, $\Delta\Delta P<0.01$ versus sh-p53 group (one-way ANOVA with Tukey's multiple comparisons test).

also significantly reduced. However, there were no significant differences in luciferase activity in the RBM4 5'-UTR-Mut2 and -Mut3 groups compared with the respective control groups. These results suggest that p53 could promote the expression of RBM4 at the transcriptional level.

AMG232 inhibits glioma angiogenesis by upregulating RBM4 expression

To further verify the role of RBM4 in the regulation of glioma angiogenesis by AMG232, RBM4-silenced GECs were constructed through stable transfection of RBM4-silencing

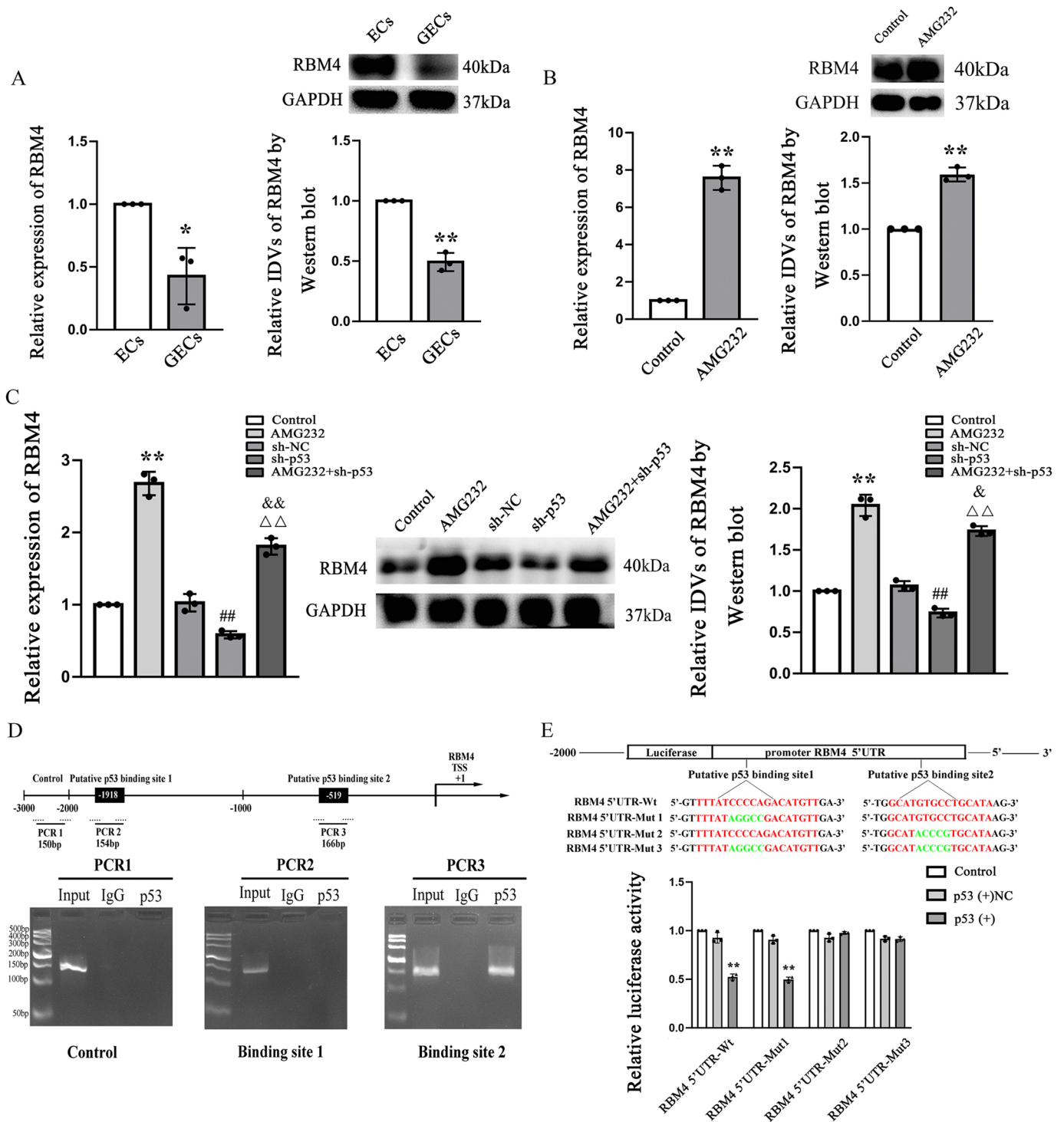


Fig. 4. AMG232 increases the expression of RBM4 by upregulating p53, which can bind to the promoter region of RBM4 to promote its expression. (A) The mRNA and protein expression levels of RBM4 in ECs and GECs were detected by qRT-PCR (left) and western blot (right) assays, respectively. Data are mean±s.d. (n=3 per group). **P*<0.05 and ***P*<0.01 versus ECs group (two-tailed unpaired Student's *t*-test). (B) The mRNA and protein expression levels of RBM4 after AMG232 treatment were detected by qRT-PCR (left) and western blot (right) assays, respectively. Data are mean±s.d. (n=3 per group). ***P*<0.01 versus control group (two-tailed unpaired Student's *t*-test). (C) qRT-PCR (left) and western blot (right) assays were used to detect the effects of p53 silencing and AMG232 alone or in combination on the mRNA and protein expression levels of RBM4. Data are mean±s.d. (n=3 per group). ***P*<0.01 versus control group, ##*P*<0.01 versus the sh-NC group, &*P*<0.05 and &&*P*<0.01 versus the AMG232 group, $\Delta\Delta$ *P*<0.01 versus the sh-p53 group (one-way ANOVA with Tukey's multiple comparisons test). (D) A ChIP assay was used to detect the binding of p53 in RBM4 promoter regions (2000 bp upstream to 100 bp downstream of the TSS). Images shown are representative of three experiments. (E) A luciferase reporter assay was conducted to detect the relationship between p53 and the target gene RBM4 promoter. The mutant sequences tested are shown in green. Data are mean±s.d. (n=3 per group). ***P*<0.01 versus p53(+)/NC group (one-way ANOVA with Tukey's multiple comparisons test).

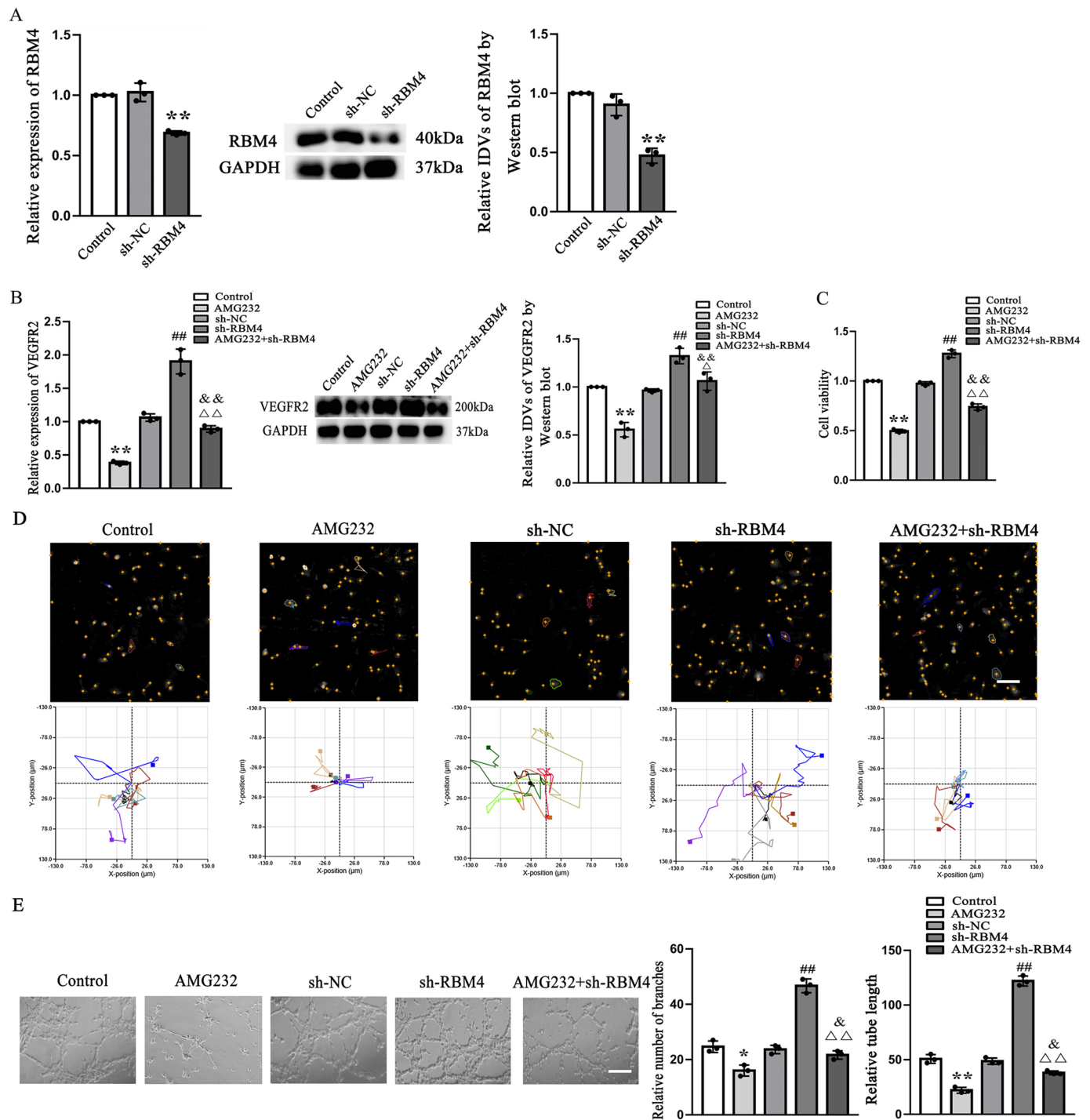


Fig. 5. The effects of RBM4 silencing on angiogenesis in GECs, and the role of RBM4 in the regulation of angiogenesis in GECs by AMG232.

(A) The silencing efficiency of RBM4 was detected by qRT-PCR (left) and western blot (right) assays. Data are mean±s.d. ($n=3$ per group). ** $P<0.01$ versus the sh-NC group (two-tailed unpaired Student's t -test). (B) The mRNA and protein expression levels of VEGFR2 in GECs were detected by qRT-PCR and western blot assay. (C) The cell viability of GECs was detected by a CCK-8 assay. (D) The Hstudio M4 system was used to observe the migration ability of GECs ($n=3$). Cell tracks are shown below the images, with the track start centered at the origin. Scale bar: 100 μm ; (E) Matrigel tube formation was conducted to verify the tube formation of GECs. Scale bar: 100 μm . Data in B, C and E are mean±s.d. ($n=3$ per group). * $P<0.05$ and ** $P<0.01$ versus control group, ### $P<0.01$ versus the sh-NC group, & $P<0.05$ and && $P<0.01$ versus the AMG232 group, $\Delta P<0.05$ and $\Delta\Delta P<0.01$ versus the sh-RBM4 group (one-way ANOVA with Tukey's multiple comparisons test).

plasmids. Silencing efficiency of RBM4 was detected and verified by qRT-PCR and western blot assays (Fig. 5A). As shown in Fig. 5B, the results of qRT-PCR and western blot assays showed that mRNA and protein expression levels of VEGFR2

were not statistically different between the sh-NC group and the control group. Compared with sh-NC group, the expression of VEGFR2 in GECs in the RBM4-silenced (sh-RBM4) group was significantly increased. Compared with AMG232 group, the

expression of VEGFR2 in GECs in the AMG232-treated and RBM4-silenced (AMG232+sh-RBM4) group was significantly increased. However, compared with the sh-RBM4 group, the expression of VEGFR2 in GECs in the AMG232+sh-RBM4 group was significantly decreased. The above results suggest that RBM4 silencing significantly upregulates VEGFR2 expression and reverses the downregulation of VEGFR2 expression by AMG232; that is, AMG232 can downregulate VEGFR2 expression by upregulating RBM4.

Similarly, as shown in Fig. 5C–E, compared with the control group, there were no significant differences in cell viability, migration ability, branch numbers and tube lengths of GECs in the sh-NC group. Compared with the sh-NC group, the cell viability and migration ability of GECs in the sh-RBM4 group were significantly enhanced, and branch numbers and tube lengths were significantly increased. Compared with AMG232 group, the cell viability and migration ability of GECs in the AMG232+sh-RBM4 group were significantly enhanced, and the branch numbers and tube lengths were significantly increased. Compared with the sh-RBM4 group, the cell viability and migration ability of GECs in the AMG232+sh-RBM4 group were significantly reduced, and the branch numbers and tube lengths were significantly decreased. The above results

suggest that RBM4 silencing significantly enhances the proliferation, migration and tube formation of GECs, and reverses the effect of AMG232 on inhibiting the proliferation, migration and tube formation of GECs. In conclusion, AMG232 could downregulate VEGFR2 expression by upregulating RBM4, thereby inhibiting the proliferation, migration and tube formation of GECs.

RBM4 binds to VEGFR2 and promotes its degradation

As shown in Fig. 6A, the results of an RBP immunoprecipitation (RIP) assay show that the expression of VEGFR2 is significantly increased in the anti-RBM4 group compared with the anti-IgG group, suggesting that RBM4 could bind to VEGFR2. In order to determine whether RBM4 regulates its expression by binding to VEGFR2, a nascent RNA capture assay was used to detect the effect of RBM4 silencing on the nascent RNA of VEGFR2. The results showed that there was no significant difference between the control group, the sh-NC group and the sh-RBM4 group, suggesting that RBM4 did not affect the nascent RNA of VEGFR2 (Fig. 6B). An actinomycin D assay was further used to detect the change of VEGFR2 half-life, as shown in Fig. 6C, compared with the control group, there was no significant difference in the half-life of VEGFR2 in the sh-NC group. Compared with the sh-NC group, the half-life of VEGFR2 in the sh-RBM4 group was

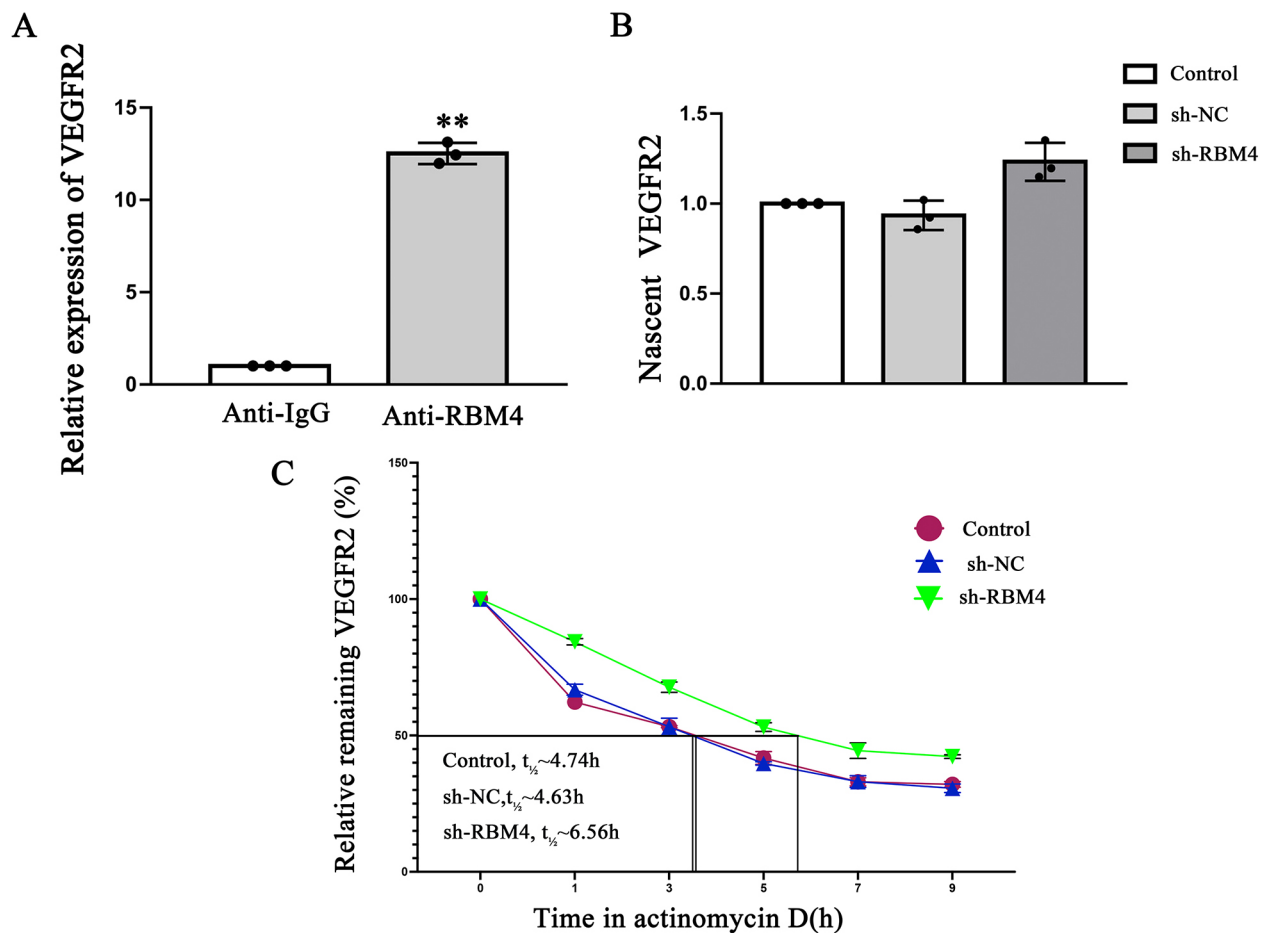


Fig. 6. RBM4 shortens its half-life by binding to VEGFR2. (A) A RIP assay verified the binding of VEGFR2 mRNA to RBM4, and a qRT-PCR assay detected the mRNA expression level of VEGFR2. Data are mean \pm s.d. ($n=3$ per group). ** $P<0.01$ versus IgG group (two-tailed unpaired Student's t -test). (B) The effect of RBM4 silencing on the nascent RNA of VEGFR2 was determined by RNA nascent capture assay. Data are mean \pm s.d. ($n=3$, per group). (C) The relative levels of the VEGFR2 in the control group, sh-NC group and sh-RBM4 group after actinomycin D treatment at different times. Data are mean \pm s.d. ($n=3$ per group).

significantly prolonged, from 4.63 h to 6.56 h, suggesting that RBM4 could bind to and shorten the half-life of VEGFR2, and promote the degradation of VEGFR2.

AMG232 regulates the expression of p53, MDM2, RBM4 and VEGFR2, and inhibits glioma angiogenesis *in vivo*

To assess the effect of AMG232 on regulating the expression of p53, MDM2, RBM4 and VEGFR2 *in vivo*, orthotopic brain glioma xenograft nude mice models were used. The results of western blot assay showed that, compared with the control group, the protein expression levels of p53 and RBM4 were increased in AMG232 group, whereas MDM2 and VEGFR2 were decreased (Fig. 7A–D). This was consistent with the results of the experiments in GECs. Meanwhile, to verify whether AMG232 inhibits GEC angiogenesis *in vivo*, a Matrigel plug assay was performed. As shown in Fig. 7E,F, the hemoglobin content in AMG232 group was decreased compared with the control group. This result demonstrated that AMG232 could inhibit glioma angiogenesis *in vivo*.

DISCUSSION

Angiogenesis, the formation of new blood vessels from pre-existing blood vessels, is a process involved in physiological conditions such as development and wound healing, but is also a key factor in many

pathological conditions, including cancer, infectious arthritis and psoriasis. It includes several steps characterized by different endothelial cell functions, such as proliferation, migration, tube formation, differentiation and maturation. Each step involves a variety of growth factors, receptors and molecules, resulting in a diversity of signaling pathways that influences the pathogenicity of angiogenesis in different diseases (Carmeliet, 2000; Unterleuthner et al., 2020). Tumor metastasis and growth depend on angiogenesis to provide oxygen, essential nutrients and metabolic functions, and angiogenesis also provides structural support for distant metastasis of tumor (Li et al., 2019). Glioblastoma is a highly vascularized tumor, and the growth of the glioma depends on the formation of new blood vessels (Balandeh et al., 2021). Studies have shown that the activation of VEGFR2 receptor on the surface of cerebral microvascular endothelial cells is the main way to promote glioma angiogenesis (Liu et al., 2018). AMG232, now also known as KRT-232, is a selective oral small molecule, currently under development for the treatment of multiple myeloma, acute myeloid leukemia (AML) and myelofibrosis (Bose and Verstovsek, 2021; Erba et al., 2019; Taylor et al., 2021). It has been reported that AMG232 is an effective MDM2 inhibitor in glioblastoma cell lines, patient-derived stem cells and multiple tumor cell lines that have wild-type *TP53*, thereby regulating tumor function, with no inhibitory effect on MDM2 in mutant *TP53* tumor cell lines (Her et al., 2018). However,

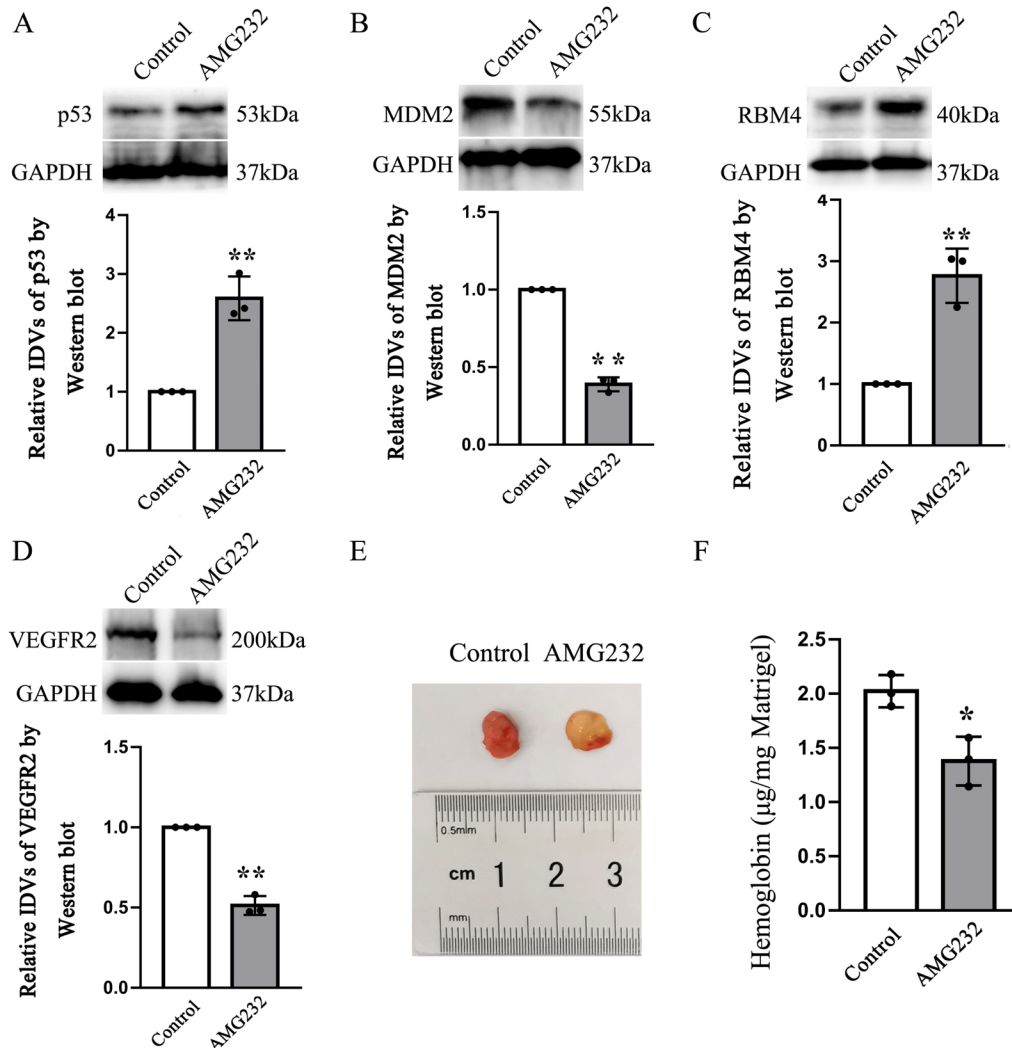


Fig. 7. The effect of AMG232 on the protein levels of p53, MDM2, RBM4 and VEGFR2, and on angiogenesis *in vivo*.

(A–D) Western blot assays were used to detect the protein levels of (A) p53, (B) MDM2, (C) RBM4 and (D) VEGFR2 after AMG232 treatment *in vivo*. Data are mean \pm s.d. ($n=3$ per group). ** $P<0.01$ versus control group (two-tailed unpaired Student's *t*-test). (E) The effect of AMG232 on glioma angiogenesis *in vivo* was tested by Matrigel plug assay. Image is representative of three experiments/mice. (F) The content of hemoglobin was detected after AMG232 treatment. Data are mean \pm s.d. ($n=3$ per group). * $P<0.05$ versus control group (two-tailed unpaired Student's *t*-test).

the effect of AMG232 on glioma angiogenesis has not been reported. In this study, p53 wild-type U87 glioma cells were co-cultured with ECs to obtain GECs. It was found that AMG232 could inhibit the proliferation of GECs in a dose-dependent manner, and 3.9 μ M AMG232 was selected to culture GECs for 48 h for subsequent studies. Furthermore, we found that AMG232 significantly inhibited the proliferation, migration and tube formation of GECs, suggesting AMG232 could inhibit angiogenesis in p53 wild-type glioma.

p53, a tumor suppressor encoded by the *TP53* gene, is a major transcriptional regulator of genes involved in apoptosis, proliferation, aging, metabolism and other cellular processes. In normal cells, the level of p53 protein is low, which is mainly caused by proteasomal degradation after polyubiquitylation mediated by ubiquitin E3 ligase MDM2 (Kubbutat et al., 1997; Haupt et al., 1997; Michael and Oren, 2003). In stressed cells, for example when there is DNA damage, the MDM2–p53 interaction is disrupted and p53 increases rapidly to activate p53 responses (Haronikova et al., 2021). The interaction between MDM2 and p53 has always played a key role in the development of tumors. For example, carcinogenic factors that result in hepatocellular carcinoma are associated with dysfunction of the MDM2–p53 axis, which presents with p53 inactivation and MDM2 overactivation (Cao et al., 2020). Our results show that p53 is expressed at low levels in GECs and MDM2 is expressed at high levels in GECs. Furthermore, AMG232 significantly upregulates the expression of p53 and downregulates the expression of MDM2 by blocking the MDM2–p53 interaction. A study has shown that activated RhoA promotes VEGF expression and hypoxia-induced angiogenesis by upregulating MDM2 and decreasing the stability of p53 (Ma et al., 2020). To clarify the role of p53 in the inhibition of angiogenesis in glioma by AMG232, the expression of p53 in GECs was silenced, and the results showed that the p53 silencing significantly upregulated the expression of VEGFR2 and promoted the proliferation, migration and tube formation of GECs. Moreover, the p53 silencing reversed the downregulation of VEGFR2 expression by AMG232 and inhibited the proliferation, migration and tube formation of GECs. Based on the above results, we believed that AMG232 could inhibit glioma angiogenesis by disrupting the MDM2–p53 interaction, thereby upregulating the expression of p53.

RBPs can regulate the target RNA at the post-transcriptional level by targeting and binding to target RNA (Tu et al., 2021). Studies have shown that RBPs are widely involved in RNA production and metabolism, and play key roles in regulating RNA stability, alternative splicing, modification, localization and translation. In a variety of cellular pathophysiological processes, the changes in the expression, structure and function of RBPs have significant impacts (Choi et al., 2018). Recent studies have shown that RBPs are involved in the occurrence and development of various tumors. For example, serine/arginine-rich splicing factor 6 (SRSF6) is highly expressed in colorectal cancer (CRC) samples and cell lines, and high expression of SRSF6 promotes the proliferation and migration of CRC cells *in vitro* and *in vivo* (Wan et al., 2019). Overexpression of QKI-5 in lung cancer cells significantly reduces the proliferation and transformation of lung cancer cells (Zong et al., 2014). As a tumor suppressor, RBM4 significantly inhibits the growth and metastasis of gastric cancer (Zhang et al., 2021). However, the role of RBM4 in the regulation of glioma angiogenesis by AMG232 has not been reported. The results of this study show that RBM4 is expressed at low levels in GECs, which is consistent with the above report that RBM4 functions as a tumor suppressor gene. Furthermore, it was found that AMG232 significantly upregulated

the expression of RBM4. p53 silencing could significantly downregulate the expression of RBM4 and reverse the upregulation of RBM4 expression by AMG232, suggesting that AMG232 increases the expression of RBM4 through upregulating p53; however, the mechanism by which p53 increases RBM4 expression remains unclear. As a transcription factor, p53 can promote or inhibit the transcription of target genes. For example, p53 can promote the expression level of Omi (also known as HtrA2) by enhancing the promoter activity of Omi (Wu et al., 2019). Therefore, we used the JASPAR and UCSC databases to analyze this and found that there were two potential p53-binding sites 2000 bp upstream and 100 bp downstream of the RBM4 TSS. ChIP and luciferase reporter gene assays confirmed that p53 could bind and transcriptionally promote the expression of RBM4; this was consistent with the research by Wu et al. (2019). These results suggest that AMG232 upregulates the expression of p53 and enhances p53-mediated RBM4 transcription, thereby inhibiting glioma angiogenesis.

More and more studies have shown that RBPs are involved in the regulation of tumor angiogenesis. For example, the expression of sterile alpha motif domain-containing 4A (SAMD4A), which is a RBP, is inhibited in breast cancer tissues and cells. Overexpression of SAMD4A inhibits the angiogenesis in breast cancer (Zhou et al., 2021). In addition, overexpression of human antigen R (HuR, also known as ELAVL1) also impairs the angiogenesis and inhibits tumor growth in triple-negative breast cancer (Gubin et al., 2010). Downregulation of FUS significantly inhibits the angiogenesis in glioma (He et al., 2019). To investigate the role of RBM4 in the regulation of glioma angiogenesis by AMG232, the expression of RBM4 in GECs was silenced. The results were similar to the above results, RBM4 silencing significantly upregulated the expression of VEGFR2 and promoted the proliferation, migration and tube formation of GECs. These results indicate that RBM4 plays an important role in regulating tumor angiogenesis and could inhibit the angiogenesis in glioma. Further studies show that RBM4 silencing reverses the downregulation of VEGFR2 expression by AMG232 and inhibits the proliferation, migration and tube formation of GECs. This proves that AMG232 inhibits glioma angiogenesis by upregulating RBM4 to inhibit the expression of VEGFR2. RBPs are key regulators of gene expression and mediate post-transcriptional regulation of gene expression mainly by binding to the 3'-UTR and 5'-UTR of target gene mRNA through specific sequences and secondary structural elements (Gerstberger et al., 2014). Ye et al. have found that RBM38 promotes the degradation of MDM2 by directly binding to its 3'-UTR in liver cancer cells (Ye et al., 2018). Studies have shown that RBM4 can participate in biological processes such as RNA translation regulation (Lin et al., 2007). Although some studies have shown that RBM4 can bind to the IRES element in the 5'-UTR region of VEGFA mRNA to regulate the translation of VEGFA (Niu et al., 2022), it has not been reported whether RBM4 can directly target and bind to VEGFR2 to regulate its expression. Through RBPmap database analysis, we found that there is a potential binding effect between RBM4 and the 3'-UTR of VEGFR2 mRNA. A RIP assay confirmed that RBM4 bound to VEGFR2. Nascent RNA capture and actinomycin D assays confirmed that RBM4 had no effect on the nascent RNA of VEGFR2, but could shorten the half-life of VEGFR2, indicating that RBM4 could bind to VEGFR2 and promote its degradation. This was consistent with the findings of Ye et al. (2018). These results confirmed that RBM4 could inhibit glioma angiogenesis by binding to VEGFR2 and promoting its degradation.

MDM2 gene amplification occurs in a variety of human malignancies, including glioma, non-small cell lung cancer and prostate cancer (Cabezón-Gutiérrez et al., 2021; Ding et al., 2019b; Feng et al., 2016). Studies have reported that MDM2 plays an important role in the regulation of tumor angiogenesis. For example, blocking MDM2 can significantly inhibit the angiogenesis of breast cancer, thereby inhibiting the growth of breast cancer (Xiong et al., 2014). MDM2 can promote the proliferation, invasion and angiogenesis of cervical cancer cells (Ding et al., 2019a). The ubiquitylation activity of MDM2 can disrupt the anti-angiogenic pathway of the p53–VHL complex, thus promoting tumor angiogenesis (Wolf et al., 2020). In glioma, MDM2 can be involved in the regulation of apoptosis and chemoresistance of glioma cells (Zhanfeng et al., 2016). The regulation of cell cycle progression by MDM2 may be related to its proliferation function in glioma cells (Dai et al., 2008). However, the roles and mechanism of MDM2 in regulating glioma angiogenesis are still unclear. Our results showed that AMG232 could significantly downregulate the expression of MDM2 in GECs, but the mechanism by which MDM2 regulates glioma angiogenesis has not been thoroughly studied. This will be the purpose of our next research because clarifying this mechanism will improve our understanding of how AMG232 inhibits angiogenesis in glioma and assist in the development of treatments for glioma.

In recent years, with the progress of cell biology and the development of three-dimensional cell cultures, *in vitro* cell lines, such as U251 and U87, are widely used in glioma genesis and development research (Xiao et al., 2017). However, because the immortal cell lines are derived from a single clone, and have adapted to the *in vitro* environment, a large number of gene mutations are present (Maqsood et al., 2013). This means that the *in vitro* experiments allow only specific aspects of tumor cells to be investigated and do not fully reflect the status of tumor cells *in vivo*. Studies have shown that after VEGFR2 is activated *in vivo*, it regulates angiogenesis through complex mechanisms. Greenberg et al. have confirmed that in ECs, VEGFR2 can promote angiogenesis after being activated by VEGF, but in vascular smooth muscle cells (VSMCs), VEGF negatively regulates the vessel maturation by promoting a receptor complex consisting of platelet-derived growth factor receptor β (PDGFR β , also known as PDGFRB) and VEGFR2 (Greenberg et al., 2008). Lu et al. have found that the VEGFR2–MET heterocomplex negatively regulates tumor cell invasion by recruiting protein tyrosine phosphatase 1B (PTP1B, also known as PTPN1) (Lu, et al., 2012). Therefore, in order to further verify the effect of AMG232 on the expression of VEGFR2 and other molecules, and its role on glioma angiogenesis, the glioma xenograft nude mice models were used. The results showed that AMG232 significantly upregulated the expression of p53 and RBM4 proteins, and downregulated the expression of MDM2 and VEGFR2 proteins in the orthotopic brain glioma xenograft nude mice. The results of an *in vivo* Matrigel plug assay showed that AMG232 significantly decreased the new vessels and the hemoglobin content. These were consistent with the results of *in vitro* experiments. Both *in vitro* and *in vivo* experimental results revealed that AMG232 inhibited glioma angiogenesis by regulating the p53–RBM4–VEGFR2 pathway.

In conclusion, this study demonstrates that p53 and RBM4 are downregulated in GECs, while MDM2 and VEGFR2 are upregulated. The *in vitro* and *in vivo* studies show that AMG232 upregulates the expression of p53 and RBM4 in GECs, and downregulates the expression of MDM2 and VEGFR2. AMG232 upregulates the expression of p53 by blocking the MDM2–p53 interaction; the upregulated p53 transcriptionally promotes the expression of RBM4,

the targets of which bind to VEGFR2 to promote its degradation, thereby inhibiting glioma angiogenesis. Our findings reveal the mechanism by which AMG232 inhibits glioma angiogenesis, and provide a new target for the diagnosis and therapy of glioma.

MATERIALS AND METHODS

Cell culture

The immortalized human cerebral microvascular endothelial cell line hCMEC/D3 was provided by Dr Couraud (Cochin Institute, Paris, France), cultured in EBM-2 medium and the endothelial medium was changed every 2 days. Each 500 ml EBM-2 medium was supplemented with 5.43 ml N-2-hydroxyethylpiperazine-N-ethane-sulphonic acid ($2\times$ HEPES), 5.43 ml chemically defined lipid concentrate, 2.75 ml ascorbic acid, 2.75 μ l hydrocortisone, 27.5 ml fetal bovine serum (FBS) and 10 ng human basic fibroblast growth factor (bFGF). The human astrocyte cell line SVG12 was purchased from Carlsbad Scientific Research Laboratory. Human U87 glioma cells were preserved in our laboratory. Human SVG12 astrocytes and human U87 glioma cells were cultured in DMEM medium with high glucose and 10% FBS was added. The medium was changed every 2 days. All cells were cultured at 37°C in a humidified incubator containing 5% CO₂ and all media were sterile filtered.

Establishment of normal human brain microvascular endothelial cells and glioma microvascular endothelial cells

Human SVG12 astrocytes and human U87 glioma cells were inoculated in 100 mm cell culture dishes, and the culture medium was changed once a day. When the cell density reached about 85%, the culture medium was discarded and washed twice with PBS, then EBM-2 culture medium was added to culture SVG12 astrocytes and U87 cells. After 1 day, the cell culture medium was collected and centrifuged at 900 g for 5 min, the supernatant was taken, and EBM-2 supplement was added to obtain astrocyte- and glioma-conditioned media. The harvested conditional medium was used to culture hCMEC/D3 to obtain ECs and GECs.

Configuration of AMG232

AMG232 powder (MedChemExpress) was dissolved in DMSO and normal saline to prepare AMG232 solutions with concentrations of 0.5 μ M, 1 μ M, 2 μ M, 4 μ M and 8 μ M (DMSO concentration was less than 0.1%).

Cell transfection

Short-hairpin p53 (sh-p53) and RBM4 (sh-RBM4) plasmids, and their corresponding negative control (sh-NC) plasmids were constructed by GenePharma Company. hCMEC/D3 cells were transfected with plasmids using Lipofectamine LTX and Plus reagent (Life) according to the manufacturer's protocol. After 26 days of G418 screening, cell lines with stable expression were selected and cultured in glioma-conditioned medium to obtain p53 and RBM4-silencing GECs. Sequences of sh-p53, sh-RBM4 and sh-NC are shown in Table S1.

Quantitative real-time PCR

Total RNA was extracted using Trizol reagent. The RNA concentration and OD260:OD280 ratio were determined using a NanoDrop spectrophotometer. Quantitative reverse transcription PCR (qRT-PCR) was performed using TB Green Premix Ex TaqII (Takara) according to the manufacturer's protocol. The reaction conditions were as follows: 25°C for 30 min, 37°C for 15 min, 85°C for 5 s and 4°C in a finite cycle. To quantify the mRNA, qPCR analysis was performed using a LightCycler 96 fluorescent quantitative PCR instrument (Roche). PCR conditions were as follows: 95°C for 30 s, 95°C for 3 s, 60°C for 30 s and 40 cycles in sequence. Using GAPDH as an endogenous control, the relative expression of target genes was calculated using the $2^{-\Delta\Delta C_t}$ method. The primers used in this study are listed in Table S2.

Western blot assay

Cells were collected and the same volume of radioimmunoprecipitation (RIPA) buffer was added (1:100 PMSF:RIPA) (Beyotime Institute of

Biotechnology) to the cells. After thorough mixing, the mixture was incubated on ice for 30 min. After ultrasonic crushing and centrifugation at 17,000 *g* at 4°C for 40 min, the supernatant was collected and the protein concentration was determined using the BCA protein assay kit (Beyotime Institute of Biotechnology). Equal amounts of protein samples were separated by electrophoresis on 10% SDS-PAGE (Beyotime Institute of Biotechnology) and transferred to PVDF membranes (Millipore). After blocking with 5% fat-free milk in Tris-buffered saline containing 0.05% Tween-20 (TTBS) at room temperature for 2 h, the membranes were incubated with primary antibodies against MDM2 (Cat No. 19058-1-AP), p53 (Cat No. 10442-1-AP), RBM4 (Cat No. 11614-1-AP), VEGFR2 (Cat No. 67407-1-Ig) and GAPDH (Cat No. 6000004-1-Ig) (1:1000, 1:2000, 1:500, 1:1000 and 1:1000, respectively; Proteintech) at 4°C overnight. After washing with TTBS, the membranes were incubated with HRP-conjugated Affinipure Goat Anti-Rabbit IgG (Cat No. SA00001-2) or HRP-conjugated Affinipure Goat Anti-Mouse IgG (Cat No. SA00001-1) secondary antibodies (diluted at 1:10,000; Proteintech) for 2 h at room temperature. Afterwards, an enhanced chemiluminescence kit (ECL; Beyotime Institute of Biotechnology) was used for luminescence, and the integrated density values (IDVs) of each band were calculated by ImageJ software. The full unedited blots are provided in Fig. S1.

Cell proliferation assay and the determination of IC₅₀

The cell viability of ECs and GECs cells were measured using the Cell Counting Kit-8 (CCK8, Dojindo). 2×10^3 cells/well were seeded in a 96-well plate, with three replicate wells in each group, and the total volume of each well was 100 μ l. The cells were placed in an incubator for pre-culture for 24 h at 37°C and 5% CO₂. Afterwards, 10 μ l of different concentrations of AMG232 were added to each well, and after incubation for a period of time (24 h, 48 h, 72 h), 10 μ l of CCK-8 solution was added to each well. The absorbance of each well was measured using a microplate reader at 450 nm after incubation for about 2 h. The absorbance value results, the cell viability and inhibition rate were calculated according to the manufacturer's protocols, and the IC₅₀ was calculated.

Cell migration assay

Cell migration ability was performed using the HoloMonitor M4 culture system (Phase Holographic Imaging) according to the manufacturer's protocols. After GECs were digested, they were pipetted evenly. The cells of each group were inoculated into a six-well plate (Corning) at a concentration of 2×10^4 cells/ml, and incubated for 12 h. After the cells adhered, the medium was replaced with 2 ml glioma-conditioned medium, placed on the HoloMonitor M4 culture system and set for imaging for 12 h at 1 h intervals. For each experimental group, we showed the last image frame and the cell movements. Five visually identified cells were randomly selected for tracking in each experimental group at the beginning of the analysis, and their movements were presented in spatial *xy* plots.

Tube formation assay

Matrigel matrix collagen solution (BD Biosciences) was thawed at 4°C overnight, 100 μ l Matrigel was added to each well of a pre-chilled 96-well plate for 10 min at 4°C, and then incubated to polymerize at room temperature for 10 min. GECs were seeded on Matrigel surface at a density of 4×10^4 cells/well and incubated at 37°C for 4 h. The images of each well were visualized using a phase contrast microscope (Olympus), and the total numbers of branches and tubule lengths were calculated using ImageJ software.

Chromatin immunoprecipitation assay

After 24 h of cells culture, GECs were washed with PBS and fixed with 1% formaldehyde for 10 min at room temperature. The crosslinking reaction was quenched by adding glycine (0.1 M), and incubated with gentle shaking for 5 min. Subsequently, the cells were washed twice with ice-cold PBS and cell lysates were prepared using ice-cold cell lysis buffer at 4°C for 1 h. The cell lysates were ultrasound treated to fragment chromatin into 500 to 800 bp lengths. The samples were pre-clarified with protein A agarose (Roche) at 4°C with gentle rotation for 1 h. Specific antibodies were then added and

kept at 4°C overnight on the rotator. To capture immune deposits, protein A agarose was blocked using salmon sperm DNA. The purified chromatin templates were amplified by PCR. The primers of each PCR set are listed in Table S3. The amplified input, IgG and IP samples were subjected to agarose gel electrophoresis.

Double luciferase reporter gene assays

The promoter region of *RBM4* was cloned into the pmirGLO plasmid, and the vector containing the p53 sequence was constructed at the same time. According to the manufacturer's protocol, cells were transfected with 50 nM pmirGLO-NC, pmirGLO-RBM4-wt or pmirGLO-RBM4-mut and 50 nM p53 or p53-NC using lipofectamine 3000. The firefly luciferase gene in the vector pmirGLO-Control was used as an endogenous control to test the transfection efficiency. After transfection for 48 h, the luciferase activities of firefly and Renilla luciferase were detected using the dual luciferase analysis reporting system. The firefly luciferase activity was normalized to the corresponding Renilla luciferase activity.

RNA-binding protein immunoprecipitation

Sufficient GECs (density above 80%) were collected with a cell scraper, centrifuged at 187 *g* for 5 min at room temperature, and precipitates were collected. 2.8 ml polysome lysis buffer 1, 2.27 μ l protease inhibitor and 8.6 μ l Rnase inhibitor were then added to blow precipitates off, then the mixture lysed on ice. 9.6 μ l Dnase salt stock and 31 μ l Dnase were added at 37°C for 10 min, then 9 μ l 0.5 M EDTA, 3.6 μ l 0.5 M EGTA and 17 μ l DTT were added in an ice bath then centrifuged at 16,000 *g* at 4°C for 14 min and the supernatant transferred to a RNase-free centrifuge tube. 10 μ l RBM4 antibody and an equal amount of IgG (1 μ g/ μ l) were added to IP and IgG samples, respectively, and incubated at 4°C for 16 h. Balanced protein A/G was added and incubated for 1 h, before washing several times. The target protein was then captured, RNA was extracted, and the concentration and quality of RNA was determined. Finally, the real-time PCR kit was used to determine the enrichment efficiency of VEGFR2.

Nascent RNA capture assay

The Click-iT NascentRNA Capture Kit (ThermoFisher Scientific) was used to measure the nascent RNA of VEGFR2. Nascent RNA in GECs was labeled with 5-ethynyluridine (EU), the cells were fixed, the EU was biotinylated using the Click reaction and the RNA-protein complexes were extracted using streptomycin affinity-coated beads. The RNA and protein were crosslinked the using UV light at 254 nm, the EU-labeled RNA-protein complexes were captured using magnetic streptavidin-binding beads, and the RNA isolated from the EU-labeled RNA-protein complexes was detected by qRT-PCR.

RNA half-life assay

Actinomycin D (5 μ g/ml) was added to the culture medium of GECs to inhibit the production of new RNA. Total RNA was extracted from GECs at 0 h, 1 h, 3 h, 5 h, 7 h and 9 h, respectively, and the expression level of VEGFR2 mRNA was detected by qRT-PCR.

Establishment of orthotopic brain glioma xenograft nude mice model

For the animal studies, a protocol detailing experimental procedures following the China Medical University guidelines was submitted to and approved by Ethics Committee of China Medical University. Eight-week-old female Balb/c nude mice were purchased from HFK Bioscience. The model was established by a method described previously (Zhang et al., 2022). A U87 glioma cell suspension, concentration $1 \times 10^6/3$ μ l, was prepared from FBS-free DMEM medium. The nude mice was anesthetized and the cell suspension was injected into the caudate nucleus of the right brain hemisphere using a Hamilton syringe and stereotaxic apparatus. Fourteen days after the tumor implantation, the xenograft nude mice were administered with AMG232 [12 mg/kg, selected according to the research (Canon et al., 2015) and our preliminary experiment results] by intraperitoneal injection. After 48 h, the brain glioma tissues were obtained for western blot assay.

In vivo Matrigel plug assay

A Matrigel plug assay was conducted to measure the angiogenesis as previously described (Würdinger et al., 2008). Four-week-old BALB/c female nude mice were used and divided into two groups: Control group and AMG232 group. Briefly, GECs resuspended in 400 ml of solution containing 80% Matrigel at a density of 3×10^5 /ml were subcutaneously injected into the right hindlimb interior root of nude mice. After 4 days, the xenograft nude mice were administered with AMG232 by intraperitoneal injection. The plugs were then removed, weighed, photographed and collected by dissolving in 400 μ m PBS (overnight incubation at 4°C). The content of hemoglobin was detected using Drabkin's solution (Sigma) according to manufacturer's directions.

Statistical analysis

SPSS (25.0) statistical software or GraphPad Prism software (7.0) were used to analyze the data, and the results are presented as mean \pm s.d. A paired Student's *t*-test was used for analysis between two groups of data, and one-way analysis of variance (ANOVA) was used for analysis between multiple groups of data. **P*<0.05 and ***P*<0.01 were considered statistically significant. All experiments were repeated three times independently.

Acknowledgements

We thank Yixue Xue, Mengyang Zhang, Yubo Zhao and Jingyi Cui for technical assistance.

Competing interests

The authors declare no competing or financial interests.

Author contributions

Conceptualization: T.M., L.L.; Investigation: Y.X., M.L., H.N.; Data curation: Y.X., H.N.; Writing - original draft: Y.X., L.L.; Writing - review & editing: L.L.; Visualization: Y.X.; Supervision: L.L.

Funding

This work was supported by grants from the Natural Science Foundation of China (81673028 to T.M. and 81402573 to L.L.) and the Natural Science Foundation of Liaoning Province of China (2019-MS-366 to L.L. and 2021-MS-158 to T.M.).

Data availability

All relevant data can be found within the article and its supplementary information.

References

- Balandeh, E., Mohammadshafie, K., Mahmoudi, Y., Hossein Pourhanifeh, M., Rajabi, A., Bahabadi, Z. R., Mohammadi, A. H., Rahimian, N., Hamblin, M. R. and Mirzaei, H. (2021). Roles of non-coding RNAs and angiogenesis in glioblastoma. *Front. Cell Dev. Biol.* **9**, 716462. doi:10.3389/fcell.2021.716462
- Bose, P. and Verstovsek, S. (2021). SOHO state of the art updates and next questions: identifying and treating "progression" in myelofibrosis. *Clin. Lymphoma Myeloma Leuk.* **21**, 641-649. doi:10.1016/j.clml.2021.06.008
- Cabezón-Gutiérrez, L., Custodio-Cabello, S., Palka-Kotłowska, M., Alonso-Viteri, S. and Khosravi-Shahi, P. (2021). Biomarkers of immune checkpoint inhibitors in non-small cell lung cancer: beyond PD-L1. *Clin. Lung Cancer* **22**, 381-389. doi:10.1016/j.clcc.2021.03.006
- Canon, J., Osgood, T., Olson, S. H., Saiki, A. Y., Robertson, R., Yu, D., Eksterowicz, J., Ye, Q., Jin, L., Chen, A. et al. (2015). The MDM2 inhibitor AMG 232 demonstrates robust antitumor efficacy and potentiates the activity of p53-inducing cytotoxic agents. *Mol. Cancer Ther.* **14**, 649-658. doi:10.1158/1535-7163.MCT-14-0710
- Cao, H., Chen, X., Wang, Z., Wang, L., Xia, Q. and Zhang, W. (2020). The role of MDM2-p53 axis dysfunction in the hepatocellular carcinoma transformation. *Cell Death Discov.* **6**, 53. doi:10.1038/s41420-020-0287-y
- Carmeliet, P. (2000). Mechanisms of angiogenesis and arteriogenesis. *Nat. Med.* **6**, 389-395. doi:10.1038/74651
- Carvalho, B., Lopes, J. M., Silva, R., Peixoto, J., Leitão, D., Soares, P., Fernandes, A. C., Linhares, P., Vaz, R. and Lima, J. (2021). The role of c-Met and VEGFR2 in glioblastoma resistance to bevacizumab. *Sci. Rep.* **11**, 6067. doi:10.1038/s41598-021-85385-1
- Chang, H.-L. and Lin, J.-C. (2019). SRSF1 and RBM4 differentially modulate the oncogenic effect of HIF-1 α in lung cancer cells through alternative splicing mechanism. *Biochim. Biophys. Acta Mol. Cell Res.* **1866**, 118550. doi:10.1016/j.bbamcr.2019.118550
- Choi, E., Oh, J., Lee, D., Lee, J., Tan, X. N., Kim, M., Kim, G., Piao, C. X. and Lee, M. (2018). A ternary-complex of a suicide gene, a RAGE-binding peptide, and polyethylenimine as a gene delivery system with anti-tumor and anti-angiogenic dual effects in glioblastoma. *J. Control. Release* **279**, 40-52. doi:10.1016/j.jconrel.2018.04.021
- Cohen, A. L. and Colman, H. (2015). Glioma biology and molecular markers. *Cancer Treat. Res.* **163**, 15-30. doi:10.1007/978-3-319-12048-5_2
- Dai, M.-S., Sun, X.-X. and Lu, H. (2008). Aberrant expression of nucleostemin activates p53 and induces cell cycle arrest via inhibition of MDM2. *Mol. Cell. Biol.* **28**, 4365-4376. doi:10.1128/MCB.01662-07
- Ding, X. Y., Jia, X. M., Wang, C., Xu, J. Y., Gao, S.-J. and Lu, C. (2019a). A DHX9-lncRNA-MDM2 interaction regulates cell invasion and angiogenesis of cervical cancer. *Cell Death Differ.* **26**, 1750-1765. doi:10.1038/s41418-018-0242-0
- Ding, Z. M., Zhang, Z. L., Jin, X., Chen, P., Lv, F., Liu, D., Shen, Y. T., Li, Y. and Gu, X. W. (2019b). Interaction with AEG-1 and MDM2 is associated with glioma development and progression and correlates with poor prognosis. *Cell Cycle* **18**, 143-155. doi:10.1080/15384101.2018.1557489
- Erba, H. P., Becker, P. S., Shami, P. J., Grunwald, M. R., Flesher, D. L., Zhu, M., Rasmussen, E., Henary, H. A., Anderson, A. A. and Wang, E. S. (2019). Phase 1b study of the MDM2 inhibitor AMG 232 with or without trametinib in relapsed/refractory acute myeloid leukemia. *Blood Adv* **3**, 1939-1949. doi:10.1182/bloodadvances.2019030916
- Feng, F. Y., Zhang, Y., Kothari, V., Evans, J. R., Jackson, W. C., Chen, W., Johnson, S. B., Luczak, C., Wang, S. M. and Hamstra, D. A. (2016). MDM2 inhibition sensitizes prostate cancer cells to androgen ablation and radiotherapy in a p53-dependent manner. *Neoplasia* **18**, 213-222. doi:10.1016/j.neo.2016.01.006
- Freedman, D. A., Wu, L. and Levine, A. J. (1999). Functions of the MDM2 oncoprotein. *Cell. Mol. Life Sci.* **55**, 96-107. doi:10.1007/s000180050273
- Gebauer, F., Schwarzl, T., Valcárcel, J. and Hentze, M. W. (2021). RNA-binding proteins in human genetic disease. *Nat. Rev. Genet.* **22**, 185-198. doi:10.1038/s41576-020-00302-y
- Gerstberger, S., Hafner, M. and Tuschl, T. (2014). A census of human RNA-binding proteins. *Nat. Rev. Genet.* **15**, 829-845. doi:10.1038/nrg3813
- Gonzalez-Rellan, M. J., Fondevila, M. F., Fernandez, U., Rodríguez, A., Varela-Rey, M., Veyrat-Durebex, C., Seoane, S., Bernardo, G., Lopitz-Otsoa, F., Fernández-Ramos, D. et al. (2021). O-GlcNAcylated p53 in the liver modulates hepatic glucose production. *Nat. Commun.* **12**, 5068. doi:10.1038/s41467-021-25390-0
- Greenberg, J. I., Shields, D. J., Barillas, S. G., Acevedo, L. M., Murphy, E., Huang, J., Scheppeke, L., Stockmann, C., Johnson, R. S., Angle, N. et al. (2008). A role for VEGF as a negative regulator of pericyte function and vessel maturation. *Nature* **456**, 809-813. doi:10.1038/nature07424
- Gubin, M. M., Calaluce, R., Davis, J. W., Magee, J. D., Strouse, C. S., Shaw, D. P., Ma, L. X., Brown, A., Hoffman, T., Rold, T. L. et al. (2010). Overexpression of the RNA binding protein HuR impairs tumor growth in triple negative breast cancer associated with deficient angiogenesis. *Cell Cycle* **9**, 3337-3346. doi:10.4161/cc.9.16.12711
- Hanahan, D. and Weinberg, R. A. (2011). Hallmarks of cancer: the next generation. *Cell* **144**, 646-674. doi:10.1016/j.cell.2011.02.013
- Haronikova, L., Bonczek, O., Zatloukalova, P., Kokas-Zavadil, F., Kucerikova, M., Coates, P. J., Fahraeus, R. and Vojtesek, B. (2021). Resistance mechanisms to inhibitors of p53-MDM2 interactions in cancer therapy: can we overcome them? *Cell. Mol. Biol. Lett.* **26**, 53. doi:10.1186/s11658-021-00293-6
- Haupt, Y., Maya, R., Kazaz, A. and Oren, M. (1997). Mdm2 promotes the rapid degradation of P53. *Nature* **387**, 296-299. doi:10.1038/387296a0
- He, Z. W., Ruan, X. L., Liu, X. B., Zheng, J., Liu, Y. H., Liu, L. B., Ma, J., Shao, L. Q., Wang, D., Shen, S. Y. et al. (2019). FUS/circ-002136/miR-138-5p/SOX13 feedback loop regulates angiogenesis in Glioma. *J. Exp. Clin. Cancer Res.* **38**, 65. doi:10.1186/s13046-019-1065-7
- Her, N.-G., Oh, J.-W., Oh, Y. J., Han, S., Cho, H. J., Lee, Y., Ryu, G. H. and Nam, D.-H. (2018). Potent effect of the MDM2 inhibitor AMG232 on suppression of glioblastoma stem cells. *Cell Death Dis.* **9**, 792. doi:10.1038/s41419-018-0825-1
- Huangfu, N., Zheng, W. Y., Xu, Z. Y., Wang, S. H., Wang, Y., Cheng, J. S., Li, Z. W., Cheng, K. A., Zhang, S. S., Chen, X. M. et al. (2020). RBM4 regulates M1 macrophages polarization through targeting STAT1-mediated glycolysis. *Int. Immunopharmacol.* **83**, 106432. doi:10.1016/j.intimp.2020.106432
- Juven-Gershon, T. and Oren, M. (1999). Mdm2: the ups and downs. *Mol. Med.* **5**, 71-83. doi:10.1007/BF03402141
- Kiang, K. M.-Y., Zhang, P. D., Li, N., Zhu, Z. Y., Jin, L. and Leung, G. K.-K. (2010). Loss of cytoskeleton protein ADD3 promotes tumor growth and angiogenesis in glioblastoma multiforme. *Cancer Lett.* **474**, 118-126. doi:10.1016/j.canlet.2020.01.007
- Konopleva, M., Martinelli, G., Daver, N., Papayannidis, C., Wei, A., Higgins, B., Ott, M., Mascarenhas, J. and Andreeff, M. (2020). MDM2 inhibition: an important step forward in cancer therapy. *Leukemia* **34**, 2858-2874. doi:10.1038/s41375-020-0949-z
- Kubbutat, M. H. G., Jones, S. N. and Vousden, K. H. (1997). Regulation of p53 stability by Mdm2. *Nature* **387**, 299-303. doi:10.1038/387299a0
- Li, S., Xu, H.-X., Wu, C.-T., Wang, W.-Q., Jin, W., Gao, H.-L., Li, H., Zhang, S.-R., Xu, J.-Z., Qi, Z.-H. et al. (2019). Angiogenesis in pancreatic cancer: current research status and clinical implications. *Angiogenesis* **22**, 15-36. doi:10.1007/s10456-018-9645-2

- Li, G., Wu, J., Li, L. and Jiang, P. (2021). p53 deficiency induces MTHFD2 transcription to promote cell proliferation and restrain DNA damage. *Proc. Natl. Acad. Sci. USA* **118**, e2019822118. doi:10.1073/pnas.2019822118
- Lin, J.-C., Hsu, M. and Tarn, W.-Y. (2007). Cell stress modulates the function of splicing regulatory protein RBM4 in translation control. *Proc. Natl. Acad. Sci. USA* **104**, 2235-2240. doi:10.1073/pnas.0611015104
- Liu, T., Ma, W. J., Xu, H. N., Huang, M. G., Zhang, D., He, Z. Q., Zhang, L., Brem, S., O'Rourke, D. M., Gong, Y. Q. et al. (2018). PDGF-mediated mesenchymal transformation renders endothelial resistance to anti-VEGF treatment in glioblastoma. *Nat. Commun.* **9**, 3439. doi:10.1038/s41467-018-05982-z
- Lu, K. V., Chang, J. P., Parachoniak, C. A., Pandika, M. M., Aghi, M. K., Meyronet, D., Isachenko, N., Fouse, S. D., Phillips, J. J., Cheresch, D. A. et al. (2012). VEGF inhibits tumor cell invasion and mesenchymal transition through a MET/VEGFR2 complex. *Cancer Cell* **22**, 21-35. doi:10.1016/j.ccr.2012.05.037
- Ma, X., Li, Z., Li, T., Zhu, L., Li, Z. and Tian, N. (2017). Long non-coding RNA HOTAIR enhances angiogenesis by induction of vegfa expression in glioma cells and transmission to endothelial cells via glioma cell derived-extracellular vesicles. *Am. J. Transl. Res.* **9**, 5012-5021.
- Ma, J., Xue, Y., Cui, W., Li, Y., Zhao, Q. L., Ye, W. M., Zheng, J., Cheng, Y. X., Ma, Y. G., Li, S. et al. (2020). Ras homolog gene family, member a promotes p53 degradation and vascular endothelial growth factor-dependent angiogenesis through an interaction with murine double minute 2 under hypoxic conditions. *Cancer* **118**, 4105-4116. doi:10.1002/cncr.27393
- Majumder, M. and Palanisamy, V. (2020). RNA binding protein FXR1-miR301a-3p axis contributes to p21WAF1 degradation in oral cancer. *PLoS Genet.* **16**, 1-25. doi:10.1371/journal.pgen.1008580
- Maqsood, M. I., Matin, M. M., Bahrami, A. R. and Ghasroldasht, M. M. (2013). Immortality of cell lines: challenges and advantages of establishment. *Cell Biol. Int.* **37**, 1038-1045. doi:10.1002/cbin.10137
- Michael, D. and Oren, M. (2003). The P53-Mdm2 module and the ubiquitin system. *Semin. Cancer Biol.* **13**, 49-58. doi:10.1016/S1044-579X(02)00099-8
- Niu, K. K., Zhang, X. J., Song, Q. S. and Feng, Q. L. (2022). G-quadruplex regulation of VEGFA mRNA translation by RBM4. *Int. J. Mol. Sci.* **23**, 743. doi:10.3390/ijms23020743
- Oliner, J. D., Kinzler, K. W., Meltzer, P. S., George, D. L. and Vogelstein, B. (1992). Amplification of a gene encoding a p53-associated protein in human sarcomas. *Nature* **358**, 80-83. doi:10.1038/358080a0
- Olivier, M., Hollstein, M. and Hainaut, P. (2010). TP53 mutations in human cancers: origins, consequences, and clinical use. *Cold Spring Harb. Perspect. Biol.* **2**, a001008. doi:10.1101/cshperspect.a001008
- Pfister, N. T., Fomin, V., Regunath, K., Zhou, J. Y., Zhou, W., Silwal-Pandit, L., Freed-Pastor, W. A., Laptenko, O., Neo, S. P., Bargonetti, J. et al. (2015). Mutant p53 cooperates with the SWI/SNF chromatin remodeling complex to regulate VEGFR2 in breast cancer cells. *Genes Dev.* **29**, 1298-1315. doi:10.1101/gad.263202.115
- Qin, J.-J., Li, X., Hunt, C., Wang, W., Wang, H. and Zhang, R. W. (2018). Natural products targeting the p53-MDM2 pathway and mutant p53: recent advances and implications in cancer medicine. *Genes Dis.* **5**, 204-219. doi:10.1016/j.gendis.2018.07.002
- Reifenberger, G., Wirsching, H.-G., Knobbe-Thomsen, C. B. and Weller, M. (2017). Advances in the molecular genetics of gliomas-implications for classification and therapy. *Nat. Rev. Clin. Oncol.* **14**, 434-452. doi:10.1038/nrclinonc.2016.204
- Sabapathy, K. and Lane, D. P. (2019). Understanding p53 functions through p53 antibodies. *J. Mol. Cell Biol.* **11**, 317-329. doi:10.1093/jmcb/mjz010
- Shibuya, M. (2013). Vascular endothelial growth factor and its receptor system: physiological functions in angiogenesis and pathological roles in various diseases. *J. Biochem.* **153**, 13-19. doi:10.1093/jb/mvs136
- Taylor, A., Lee, D., Allard, M., Poland, B. and Greg Slatter, J. (2021). Phase 1 concentration-QTc and cardiac safety analysis of the MDM2 antagonist KRT-232 in patients with advanced solid tumors, multiple myeloma, or acute myeloid leukemia. *Clin. Pharmacol. Drug Dev.* **10**, 918-926. doi:10.1002/cpdd.903
- Tu, Z. W., Shu, L., Li, J. Y., Wu, L., Tao, C. M., Ye, M. H., Zhu, X. G. and Huang, K. (2021). A novel signature constructed by RNA-binding protein coding genes to improve overall survival prediction of glioma patients. *Front. Cell Dev. Biol.* **8**, 588368. doi:10.3389/fcell.2020.588368
- Unterleuthner, D., Neuhold, P., Schwarz, K., Janker, L., Neuditschko, B., Nivarthi, H., Crncec, I., Kramer, N., Unger, C., Hengstschläger, M. et al. (2020). Cancer-associated fibroblast-derived WNT2 increases tumor angiogenesis in colon cancer. *Angiogenesis* **23**, 159-177. doi:10.1007/s10456-019-09688-8
- Wan, L., Yu, W. Y., Shen, E. H., Sun, W. J., Liu, Y., Kong, J. L., Wu, Y. H., Han, F. Y., Zhang, L., Yu, T. Z. et al. (2019). SRSF6-regulated alternative splicing that promotes tumour progression offers a therapy target for colorectal cancer. *Gut* **68**, 118-129. doi:10.1136/gutjnl-2017-314983
- Wang, W.-Y., Quan, W., Yang, F., Wei, Y.-X., Chen, J.-J., Yu, H., Xie, J., Zhang, Y. and Li, Z.-F. (2020). RBM4 modulates the proliferation and expression of inflammatory factors via the alternative splicing of regulatory factors in HeLa cells. *Mol. Genet. Genomics* **295**, 95-106. doi:10.1007/s00438-019-01606-3
- Wolf, E. R., Mabry, A. R., Damania, B. and Mayo, L. D. (2020). Mdm2-mediated neddylation of pVHL blocks the induction of antiangiogenic factors. *Oncogene* **39**, 5228-5239. doi:10.1038/s41388-020-1359-4
- Wu, L. G., Liu, D., Wu, Y., Wei, X., Wang, Z. J., Wang, W., Zhang, S. L., Yang, H., Yi, M. and Liu, H. R. (2019). p53 mediated transcription of Omi/HtrA2 in aging myocardium. *Biochem. Biophys. Res. Commun.* **519**, 734-739. doi:10.1016/j.bbrc.2019.09.062
- Würdinger, T., Tannous, B. A., Saydam, O., Skog, J., Grau, S., Soutschek, J., Weissleder, R., Breakefield, X. O. and Krichevsky, A. M. (2008). miR-296 regulates growth factor receptor overexpression in angiogenic endothelial cells. *Cancer Cell* **14**, 382-393. doi:10.1016/j.ccr.2008.10.005
- Xiao, W., Sohrobi, A. and Seidlits, S. K. (2017). Integrating the glioblastoma microenvironment into engineered experimental models. *Future Sci.* **3**, FSO189. doi:10.4155/fsoa-2016-0094
- Xiong, J., Yang, Q., Li, J. S. and Zhou, S. (2014). Effects of MDM2 inhibitors on vascular endothelial growth factor-mediated tumor angiogenesis in human breast cancer. *Angiogenesis* **17**, 37-50. doi:10.1007/s10456-013-9376-3
- Xu, S. C., Tang, L., Li, X. Z., Fan, F. and Liu, Z. X. (2020). Immunotherapy for glioma: Current management and future application. *Cancer Lett.* **476**, 1-12. doi:10.1016/j.canlet.2020.02.002
- Ye, J., Liang, R., Bai, T., Lin, Y., Mai, R., Wei, M., Ye, X., Li, L. and Wu, F. (2018). RBM38 plays a tumor-suppressor role via stabilizing the p53-mdm2 loop function in hepatocellular carcinoma. *J. Exp. Clin. Cancer Res.* **37**, 212. doi:10.1186/s13046-018-0852-x
- Zhanfeng, N., Chengquan, W., Hechun, X., Jun, W., Lijian, Z., Dede, M., Wenbin, L. and Lei, Y. (2016). Period2 downregulation inhibits glioma cell apoptosis by activating the MDM2-TP53 pathway. *Oncotarget* **7**, 27350-27362. doi:10.18632/oncotarget.8439
- Zhang, Y., Yong, H. M., Fu, J., Gao, G. Y., Shi, H. C., Zhou, X. Y. and Fu, M. S. (2021). miR-504 promoted gastric cancer cell proliferation and inhibited cell apoptosis by targeting RBM4. *J. Immunol. Res.* **2021**, 5555950. doi:10.1155/2021/5555950
- Zhang, M., Yang, C., Ruan, X., Liu, X., Wang, D., Liu, L., Shao, L., Wang, P., Dong, W. and Xue, Y. (2022). CPEB2 m6A methylation regulates blood-tumor barrier permeability by regulating splicing factor SRSF5 stability. *Commun Biol* **5**, 908. doi:10.1038/s42003-022-03878-9
- Zhou, M. C., Wang, B., Li, H. W., Han, J. Q., Li, A. L. and Lu, W. B. (2021). RNA-binding protein SAMD4A inhibits breast tumor angiogenesis by modulating the balance of angiogenesis program. *Cancer Sci.* **112**, 3835-3845. doi:10.1111/cas.15053
- Zong, F.-Y., Fu, X., Wei, W.-J., Luo, Y.-G., Heiner, M., Cao, L.-J., Fang, Z. Y., Fang, R., Lu, D. R., Ji, H. B. et al. (2014). The RNA-binding protein QKI suppresses cancer-associated aberrant splicing. *PLoS Genet.* **10**, e1004289. doi:10.1371/journal.pgen.1004289